

Quantum phase transition and criticality in quasi one-dimensional spinless Dirac fermions

Yasuhiro Tada^{1,*}

¹*Institute for Solid State Physics, University of Tokyo, Kashiwa 277-8581, Japan*

We study quantum criticality of spinless fermions on the quasi one dimensional π -flux square lattice in cylinder geometry, by using the infinite density matrix renormalization group and abelian bosonization. For a series of the cylinder circumferences $L_y = 4n + 2 = 2, 6, \dots$ with the periodic boundary condition, there are quantum phase transitions from gapped Dirac fermion states to charge density wave (CDW) states. We find that the quantum phase transitions for such circumferences are continuous and belong to the (1+1)-dimensional Ising universality class. On the other hand, when $L_y = 4n = 4, 8, \dots$, there are gapless Dirac fermions at the non-interacting point and the phase transition to the CDW state is Gaussian. Both of these two criticalities are described in a unified way by the bosonization. We clarify their intimate relationship and demonstrate that a central charge $c = 1/2$ Ising transition line arises as a critical state of an emergent Majorana fermion from the $c = 2$ Gaussian transition point.

I. INTRODUCTION

Criticality associated with a phase transition is one of the central issues in condensed matter physics. Various phase transitions have been established mainly for insulators which are well described by bosonic models such as Ising, XY, and Heisenberg models. However, phase transitions in *metals* where gapless fermions are coupled with bosons are rather poorly understood compared to insulators only with bosons. In such a system, fermions strongly affect low energy behaviors of the bosonic order parameters and consequently could change criticality of the phase transition. The critical bosonic fluctuations in turn influence the fermions, and resulting non-Fermi liquid like behaviors are often observed in various systems¹⁻⁴.

The criticality depends on structures of fermionic excitations such as dimensionality of the Fermi surface and the number of fermion flavors (orbitals and spins). One of the simplest examples is the spinless fermions on a one-dimensional (1D) chain at half-filling with the nearest neighbor repulsive interaction V , where the classical ground states for $V \rightarrow \infty$ are the charge density wave (CDW) states^{5,6}. When one introduces fermionic hopping t , there will be a Kosterlitz-Thouless phase transition to a Tomonaga-Luttinger liquid, which is distinct from the Ising transition in bosonic models such as the transverse Ising model. Quantum criticality in higher dimensional systems are also of great interest, and in this context, a semi-metallic system is an ideal platform to study interplay between fermions and bosons where the Fermi surface is a point. Indeed, critical behaviors of phase transitions in Dirac systems have been extensively studied, and the gapless Dirac excitations can lead to new criticalities such as chiral Ising, chiral XY, chiral Heisenberg universality classes⁷⁻²². The critical exponents of these phase transitions have been evaluated accurately by several methods, e.g. analytical calculations and unbiased quantum Monte Carlo simulations. In these (semi)metallic systems, the gapless fermions play essen-

tial roles and the resulting quantum criticality is different from that in the corresponding purely bosonic system with gapped fermions.

These two criticalities are usually studied separately as distinct properties of metals and insulators. For example, the quantum phase transition from a gapless Dirac state to an antiferromagnetic state in a honeycomb lattice is described by (2+1)D chiral Heisenberg universality class, while the one from a spin-orbit coupled gapped Dirac state to the antiferromagnetic state belongs to 3D XY universality class^{13,23,24}. Similarly, one can separately discuss two criticalities of phase transitions from a metal or a band insulator to an ordered state in general. However, such separate discussions would be somewhat subtle when the band gap is very small, and there will be crossover between fermionic criticality and bosonic criticality in a narrow gap system. Then, a natural question is that how these two criticalities are connected along the critical line of the phase transition in an extended phase diagram including both metals and insulators (Fig. 1).

In this study, we consider quasi 1D half-filled spinless fermions on a π -flux square lattice in cylinder geometry with the circumference L_y , as a simple example for the quantum phase transition of \mathbb{Z}_2 symmetry breaking. When the nearest neighbor repulsive interaction V is weak, there are Dirac fermions with a mass m due to the finite system size L_y for $L_y = 2, 6, 10, \dots$ under the periodic boundary condition along the y -direction, while there are gapless Dirac fermions at $V = 0$ for $L_y = 4n = 4, 8, \dots$. The system exhibits a staggered CDW ordered state for large V . The quantum phase transition is studied with use of the infinite density matrix renormalization group (iDMRG)²⁵⁻³⁰ together with the recently developed scaling analysis¹⁶. Then, we demonstrate that the quantum phase transition at a critical $V = V_c > 0$ between the gapped Dirac fermions and the CDW state is continuous, and the corresponding criticality is simply (1+1)D Ising universality class. On the other hand, the iDMRG results suggest that the phase transition from the gapless Dirac state is smooth

around $V = 0$, which turns out to be Gaussian. These two behaviors are well described within the bosonization approach in a unified manner, and a global phase diagram in the V - m plane is discussed. We clarify their intimate relationship and demonstrate that the central charge $c = 1/2$ Ising transition line arises as a critical state of an emergent Majorana fermion from the $c = 2$ Gaussian transition point.

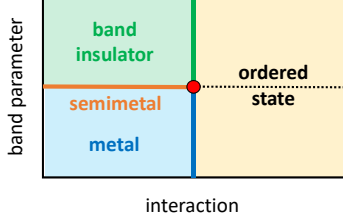


FIG. 1. A schematic phase diagram including both insulating and (semi)metallic states. Generally, the blue and green phase transition lines and the red transition point would be characterized by different criticalities.

II. MODEL AND PHASE TRANSITION

A. Model

We consider spinless fermions on a π -flux square lattice at half-filling,

$$H = - \sum_{\langle i,j \rangle} t_{ij} c_i^\dagger c_j + V \sum_{\langle i,j \rangle} n_i n_j, \quad (1)$$

where $t_{ij} = t(-t)$ along the x -direction at even (odd) y_i and $t_{ij} = t$ along the y -direction. $\langle i, j \rangle$ represents a pair of nearest neighbor sites (Fig. 2). We use the energy unit $t = 1$. The system size is $L_x \times L_y = \infty \times L_y$ with the periodic boundary condition for the y -direction otherwise specified. In 2D ($L_y = \infty$) at $V = 0$, this model has two Dirac points and there is a continuous quantum phase transition to a staggered CDW state at $V_c \simeq 1.30t^{9-12}$. The criticality of the CDW phase transition belongs to the (2+1)D chiral Ising universality class, whose critical exponents are evaluated as $\beta \simeq 0.60 \pm 0.07$ and $\nu \simeq 0.79 \sim 0.80$ by the quantum Monte Carlo calculations⁹⁻¹².

For a finite $L_y > 2$, the single particle dispersion under the periodic boundary condition for the y -direction is given by

$$\varepsilon(k_x, k_y) = \pm \sqrt{(2t \cos k_x)^2 + (2t \cos k_y)^2}, \quad (2)$$

where k_x takes continuum values and $k_y = 2\pi n/L_y$, ($n = 0, 1, \dots, L_y/2 - 1$). Similarly, $\varepsilon(k_x) = \pm \sqrt{(2t \cos k_x)^2 + t^2}$ for $L_y = 2$. Due to the discreteness of k_y , the dispersion is qualitatively different when $L_y = 4n = 4, 8, 12, \dots$ and

$L_y = 4n + 2 = 2, 6, 10, \dots$; the gapless Dirac points exist for $L_y = 4n$, while the Dirac fermions are massive with the gap size $m \sim t_y/L_y$ for $L_y = 4n + 2$. $\varepsilon(k)$ is shown in Fig. 3 for $L_y = 8$ and $L_y = 10$ as an example.

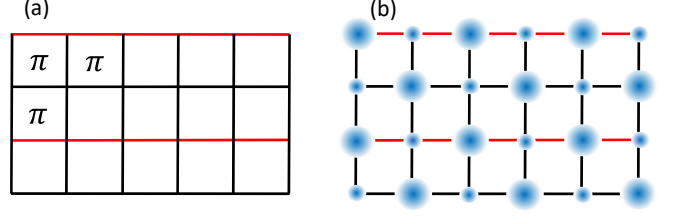


FIG. 2. (a) A $L_y = 4$ π -flux square lattice. The hopping on the black bonds is $-t$ and that on the red bonds is $+t$, which gives a π -flux for each square plaquette. (b) Schematic picture of the staggered CDW order. The blue circles represent the fermion particle density.

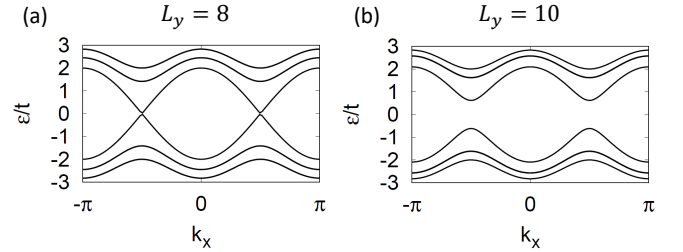


FIG. 3. Single particle dispersion relations (a) for $L_y = 8$ and (b) for $L_y = 10$ under the periodic boundary condition in the y -direction.

To discuss effects of the interaction V , we use iDMRG for a system of cylinder geometry and abelian bosonization. The iDMRG allows a highly accurate calculation, and has been used extensively not only for one dimensional systems but also for two dimensional systems. One can directly describe a quantum phase transition of discrete symmetry in such an infinite length cylinder by using iDMRG. Later, we also perform bosonization analysis around $V = 0$ but with a twisted boundary condition for the y -direction, which enables us to discuss the gapped and gapless fermions on an equal footing.

B. iDMRG calculations

1. Order parameter

In this section, the CDW quantum phase transition is investigated by iDMRG²⁵⁻²⁸ with use of the open source code TenPy^{29,30}. We discuss the CDW order parameter associated with the \mathbb{Z}_2 symmetry breaking,

$$\Delta = \frac{1}{L'_x L_y} \sum_i (-1)^{|i|} n_i, \quad (3)$$

where L'_x is the unit period assumed in the iDMRG calculation. The summation is over $x = 1, 2, \dots, L'_x$ and $y = 1, 2, \dots, L_y$. We have performed calculations for various L'_x and confirmed that the results are essentially independent of L'_x . Firstly, we show $|\Delta|$ for the massive case ($L_y = 4n + 2$) and massless case ($L_y = 4n$) respectively in Fig. 4. For the massive case $L_y = 2, 6, 10, 14$, we find a clear quantum phase transition from the gapped Dirac state to the CDW state at L_y -dependent critical values $V = V_c(L_y) > 0$. The critical value $V_c(L_y)$ decreases as L_y increases for a fixed bond dimension χ , because the Dirac band mass $m \sim t_y/L_y$ is reduced for larger L_y . We expect that $V_c(L_y)$ is monotonically decreasing and approaches the 2D value $V_c(\infty) = 1.30$, although $V_c(14)$ for χ used is smaller than $V_c(\infty)$ due to the strong finite χ effect. On the other hand, for the massless case with $L_y = 4, 8, 12$, the order parameter Δ behaves smoothly as a function of V since the gapless Dirac states can be correctly described only when the bond dimension χ in the iDMRG calculation is infinitely large $\chi \rightarrow \infty$. In this limit, we expect a Gaussian transition takes place at $V = 0$, which is indeed described by the bosonization in the later section. In the next part, we focus on the massive case $L_y = 4n + 2$ and discuss its criticality within iDMRG.

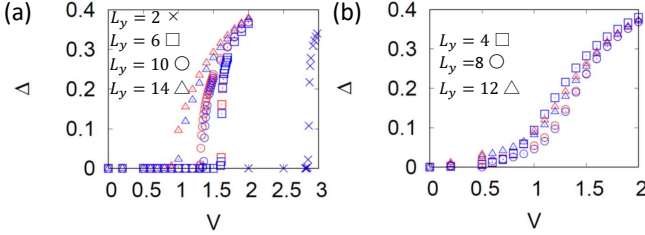


FIG. 4. The CDW order parameter Δ as a function of the interaction V calculated by iDMRG with the periodic boundary condition for the y -direction. (a) $L_y = 4n + 2 = 6, 10, 14$ with $\chi = 1000$ (red), 1600 (blue). For $L_y = 2$, $\chi = 100$ (red), 200 (blue). (b) $L_y = 4n = 4, 8, 12$ with $\chi = 1000$ (red), 1600 (blue). Note that the data for $L_y = 2, 4$ with the different values of χ almost coincide in the present scale of the figures.

2. Finite correlation length scaling for $L_y = 4n + 2$

The criticality of the phase transition for $L_y = 4n + 2 = 2, 6, 10, \dots$ is expected to be (1+1)D Ising universality class if it is continuous, because the CDW state breaks \mathbb{Z}_2 translation symmetry and there is no gapless Dirac fermions at $V = 0$ for these L_y . In order to examine the criticality numerically, we use the scaling ansatz recently developed for tensor network states in iPEPS¹⁶. Since the one-dimensional system size L_x is infinite in iDMRG, criticality is controlled not by $L_x = \infty$ but by the correlation length ξ_χ in our calculations. The correlation length ξ_χ is computed from the second largest

eigenvalue of the transfer matrix for a given bond dimension χ , and ξ_χ characterizes finite bond dimension effects. One would naively expect that the system may exhibit the (2+1)D χ -Ising criticality if $\xi_\chi \ll L_y$, while it shows (1+1)D bosonic Ising criticality if $\xi_\chi \gg L_y$. In the following, we focus only on the latter case with $\xi_\chi \gg L_y$.

The scaling ansatz for the ground state energy density is written as

$$E(g, h, \xi_\chi^{-1}) = b^{-2} E(b^{y_g} g, b^{y_h} h, b \xi_\chi^{-1}), \quad (4)$$

where $g = (V - V_c(L_y))/V_c(L_y)$ and h is the conjugate field to Δ . We have assumed the dynamical critical exponent is $z = 1$. The L_y -dependent critical points $V_c(L_y)$ are determined so that a scaling behavior of the order parameter Eqs. (5), (6) hold for larger ξ_χ . We obtain $V_c(L_y = 2) \simeq 2.8686$, $V_c(6) \simeq 1.624$, and $V_c(10) \simeq 1.50$ as will be discussed in the following. At the critical point $g = 0$, the CDW order parameter exhibits the scaling behaviors

$$\Delta(g = 0) \sim \xi_\chi^{-\beta/\nu}, \quad (5)$$

$$\frac{\partial_g \Delta(g = 0)}{\Delta(0)} \sim \xi_\chi^{1/\nu}, \quad (6)$$

which are derived from the scaling ansatz Eq.(4). From these two equations, we can determine the critical exponents β and ν .

In Fig. 5, we show ξ_χ -dependence of Δ and $\partial_g \Delta/\Delta$ for $L_y = 2$. First of all, the quantum phase transition is continuous since the scaling behaviors hold up to large $\xi_\chi > 1000$, although a discontinuous transition was potentially possible. The critical interaction strength is obtained as $V_c(L_y = 2) = 2.8686$ from the figure. The critical behaviors of Δ are in good agreement with those of (1+1)D Ising universality class with $\beta = 0.125, \nu = 1$, as we have expected. Similarly, we show ξ_χ -dependence of Δ and $\partial_g \Delta/\Delta$ for $L_y = 6$ in Fig. 6. The critical interaction is evaluated as $V_c(L_y = 6) = 1.624$. Although there is some signature for dimensional crossover from (2+1)D chiral Ising universality class for small $\xi_\chi \lesssim L_y$, the true criticality close to the critical point $g = 0$ belongs to the (1+1)D Ising universality class. For $L_y = 10$, however, it is difficult to explicitly demonstrate the critical behavior of the (1+1)D Ising universality class as shown in Fig. 7, because of the heavy finite χ effects. Here, we used χ up to 2400, and the critical interaction is estimated to be $V_c(L_y = 10) \simeq 1.50$. We think that the critical behavior of the (1+1)D Ising universality class will be reproduced for sufficiently large χ similarly to the cases for $L_y = 2, 6$.

To further confirm the critical behaviors of the (1+1)D Ising universality class, in Fig. 8, we show the scaling plot

$$\Delta \xi_\chi^{\beta/\nu} = \mathcal{M}(g \xi_\chi^{1/\nu}), \quad (7)$$

where \mathcal{M} is a scaling function. Here, we have used only the data for $\xi_\chi > L_y$ to avoid effects of the dimensional crossover. All the data collapse into a single curve in each system size $L_y = 2, 6$, which gives a cross check

for the Ising universality class of the CDW phase transition. Finally, Fig 9 shows the entanglement entropy S for bipartitioning the infinite one dimensional chain in the iDMRG calculation into two half-infinite chains. In such bipartitioning, the entanglement entropy at the critical point is characterized by the central charge c of the underlying conformal field theory and is given by

$$S = \frac{c}{6} \ln \xi_\chi + S_0, \quad (8)$$

where S_0 is a constant^{29,31}. In the present system, the calculated S at the critical point is well fitted by this formula with $c = 1/2$, which means that the corresponding conformal field theory is the $c = 1/2$ Ising theory in agreement with the critical behaviors of the order parameter Δ .

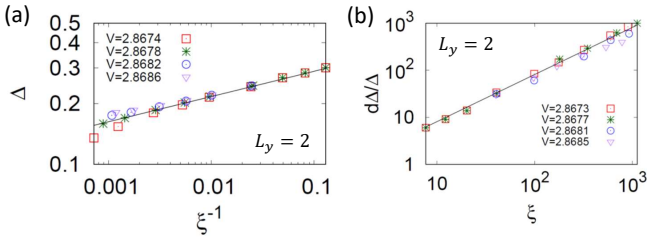


FIG. 5. The scaling plots of the CDW order parameter for $L_y = 2$. The correlation length ξ_χ is denoted as ξ for simplicity. (a) The scaling plot Eq. (5), and the black line is $\Delta \sim \xi^{-\beta/\nu}$ with $\beta = 0.125, \nu = 1$. (b) The scaling plot Eq. (6), and the black line is $\partial_g \Delta / \Delta \sim \xi^{1/\nu}$ with $\nu = 1$. The g -derivative is approximated by $\partial_g \Delta(V) = V_c [\Delta(V + \delta V) - \Delta(V - \delta V)] / \delta V$ with $\delta V = 0.0001$. The bond dimension is used up to $\chi \leq 200$.

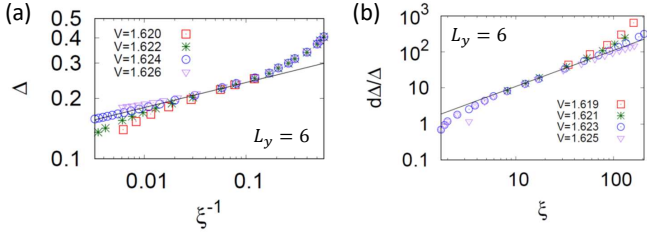


FIG. 6. The scaling plots of the CDW order parameter for $L_y = 6$. (a) The scaling plot Eq. (5) and (b) Eq. (6). The black lines are the same as in Fig. 5, while the g -derivative is approximated with $\delta V = 0.001$. The bond dimension is used up to $\chi \leq 2800$.

C. Bosonization and global phase diagram

In this section, we discuss the relationship between the CDW phase transitions from gapless and gapped Dirac states within the bosonization approach^{5,6,32,33}. Our primary purpose is to find an effective theory description for the iDMRG calculation results. To discuss the gapless

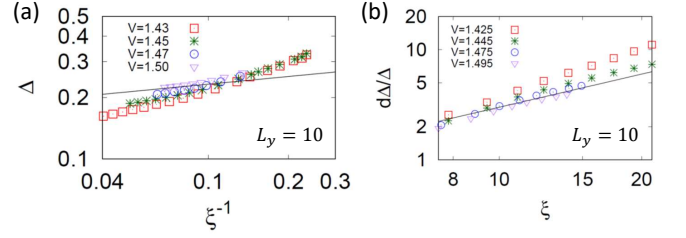


FIG. 7. The scaling plots of the CDW order parameter for $L_y = 10$. (a) The scaling plot Eq. (5) and (b) Eq. (6). The black lines are the same as in Fig. 5, while the g -derivative is approximated with $\delta V = 0.005$. The bond dimension is used up to $\chi \leq 2400$.

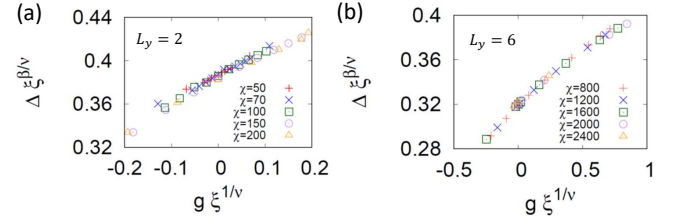


FIG. 8. The scaling plot of the CDW order parameter Δ for (a) $L_y = 2$ and (b) $L_y = 6$. The critical exponents used are those for the (1+1)D Ising universality class $\beta = 0.125, \nu = 1$.

and gapped states on an equal footing, we introduce the twisted boundary condition with the twist angle θ for the y -direction, or equivalently insert a flux θ along the cylinder³⁴. When $\theta = 0$ the boundary condition is realized and the non-interacting Dirac fermions are gapless for $L_y = 4n$. The band gap in Eq. (2) is tuned by the twisting angle θ since the allowed discrete $k_y (= (2\pi n + \theta)/L_y)$ points for given finite L_y changes as θ is varied. For example in $L_y = 4n$ case, the band gap becomes maximum at $\theta = \pi$, for which there is a CDW phase transition from a gapped Dirac state whose criticality is (1+1)D Ising universality class. In this way, one can smoothly connect the two extreme cases, the gapless Dirac semimetal and maximally gapped Dirac band insulator, for fixed system size L_y .

We firstly consider the non-interacting excitation spectra in the π -flux cylinder for example with a fixed $L_y =$

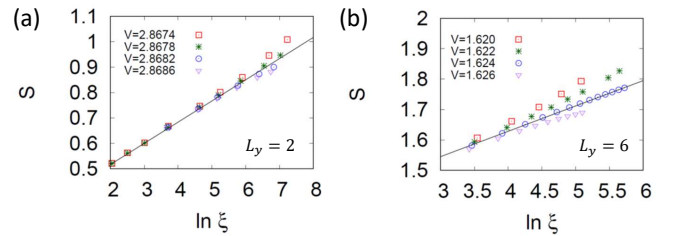


FIG. 9. The entanglement entropy S for (a) $L_y = 2$ and (b) $L_y = 6$. The black lines are $S = (c/6) \ln \xi + S_0$ with the central charge $c = 1/2$.

$4n$ under the periodic boundary condition as shown in Fig. 3 (a), and focus only on the gapless Dirac fermion branches and neglect other gapped bands. There are two pairs of linear dispersions with positive and negative velocities around $k_x = \pm\pi/2$. If we introduce a twist angle θ , a band gap $m(\theta)$ will be induced in the pre-existing gapless Dirac bands. The two branches can be reproduced by an effective two leg ladder model

$$H_{\text{eff}} = \sum_{s=1,2} \sum_i -t_s c_{is}^\dagger c_{i+1s} - t_\perp \sum_i c_{i1}^\dagger c_{i2} + (\text{h.c.}) \\ + \tilde{U} \sum_i n_{i1} n_{i2} + \tilde{V} \sum_{s=1,2} \sum_i n_{is} n_{i+1s}, \quad (9)$$

where $t_s = (-1)^{s+1}t$, $t_\perp = 2t|\sin\theta|$, $\tilde{U} = 2V/L_y$, $\tilde{V} = V/L_y$. A similar effective model was studied before in the context of carbon nanotubes³². By using the transformation $c_{i1} \rightarrow c_{i1}$, $c_{i2} \rightarrow (-1)^i c_{i2}$, the Hamiltonian is rewritten into the familiar form with an additional staggered hybridization term $(-1)^i t_\perp$,

$$H_{\text{eff}} \rightarrow \sum_{s=1,2} \sum_i -t c_{is}^\dagger c_{i+1s} - t_\perp \sum_i (-1)^i c_{i1}^\dagger c_{i2} + (\text{h.c.}) \\ + \tilde{U} \sum_i n_{i1} n_{i2} + \tilde{V} \sum_{s=1,2} \sum_i n_{is} n_{i+1s}, \quad (10)$$

where hopping along the chain is t for both $s = 1, 2$.

The fermion operators are approximated around the Fermi point $k_F = \pm\pi/2a$ as $\psi_s(x) = e^{-ik_F x} \psi_{Ls}(x) + e^{ik_F x} \psi_{Rs}(x)$ with $\psi_{rs}(x) = \eta_{rs} e^{-i(r\phi_s - \theta_s)}/\sqrt{2\pi a}$, where a is the lattice constant and η_{rs} is the Klein factor^{5,6}. The bosonic phase operators satisfy the commutation relation

$$[\phi_s(x), \partial_{x'} \theta_{s'}(x')] = i\pi \delta_{ss'} \delta(x - x'). \quad (11)$$

Furthermore, we introduce new fields $\phi_{0,\pi} = (\phi_1 \pm \phi_2)/\sqrt{2}$ for convenience. Then the Hamiltonian is bosonized into

$$H_{\text{eff}} = H_{\text{kin}} + H_{\text{int}}, \quad (12)$$

$$H_{\text{kin}} = \sum_{k=0,\pi} \frac{v_k}{2\pi} \int dx [K_k^{-1} (\partial\phi_k)^2 + K_k (\partial\theta_k)^2],$$

$$H_{\text{int}} = \int dx [g_1 \cos \sqrt{8}\phi_0 + g_2 \cos \sqrt{8}\phi_\pi \\ + g_3 \cos \sqrt{8}\phi_0 \cos \sqrt{8}\phi_\pi + g_4 \cos \sqrt{2}\phi_0 \sin \sqrt{2}\theta_\pi],$$

where $g_1 = -\tilde{U}/2\pi^2 a$, $g_2 = \tilde{U}/2\pi^2 a$, $g_3 = \tilde{V}/\pi^2 a$, $g_4 = 2t_\perp/\pi a$. For small \tilde{U}, \tilde{V} , the parameters are given by $v_0 = v_F/K_0$, $v_\pi = v_F/K_\pi$, and

$$K_0^{-1} = \sqrt{1 + \frac{a}{\pi v_F} (\tilde{U} + 4\tilde{V})} \simeq 1 + \frac{a}{2\pi v_F} (\tilde{U} + 4\tilde{V}), \quad (13a)$$

$$K_\pi^{-1} = \sqrt{1 + \frac{a}{\pi v_F} (-\tilde{U} + 4\tilde{V})} \simeq 1 + \frac{a}{2\pi v_F} (-\tilde{U} + 4\tilde{V}), \quad (13b)$$

where $v_F = 2t$ is the Fermi velocity of the non-interacting model. The scaling dimensions of the operators are easily read off as

$$[g_1] = 2K_0 \simeq 2 - \frac{a}{\pi v_F} (\tilde{U} + 4\tilde{V}), \quad (14a)$$

$$[g_2] = 2K_\pi \simeq 2 - \frac{a}{\pi v_F} (-\tilde{U} + 4\tilde{V}), \quad (14b)$$

$$[g_3] = 2K_0 + 2K_\pi \simeq 4 - \frac{8a}{\pi v_F} \tilde{V}, \quad (14c)$$

$$[g_4] = \frac{K_0}{2} + \frac{1}{2K_\pi} \simeq 1 - \frac{a}{2\pi v_F} \tilde{U}. \quad (14d)$$

We first consider the case with $t_\perp = 0$, or equivalently $g_4 = 0$. Then, the most relevant term is the g_1 -term, and ϕ_0 -field gets pinned to $\langle\phi_0\rangle = 0$ because of the strong coupling $g_1 \rightarrow -\infty$. The remaining g_2, g_3 -terms will have the same functional form, $\cos \sqrt{8}\phi_\pi$, and be renormalized to $g_2, g_3 \rightarrow \infty$. Therefore, both of the two fields ϕ_0, ϕ_π become gapped as long as $V > 0$, and the phase transition is a Gaussian transition from the $c = 2$ two-flavor gapless Dirac state to the fully gapped CDW state. This is consistent with the iDMRG calculation where the CDW order parameter is non-zero for very small V when $L_y = 4n = 4, 8, \dots$ under the periodic boundary condition.

Next, we consider a very small $0 < t_\perp \ll V$, for which the renormalized parameters still satisfy $|g_4| \ll |g_1|$ down to some energy scale under the renormalization group. In this energy scale, ϕ_0 -field is nearly locked as $\langle\phi_0\rangle \simeq 0$ and the low energy physics is described by the ϕ_π -field only,

$$H_{\text{eff}} \simeq \frac{v_\pi}{2\pi} \int dx [K_\pi^{-1} (\partial\phi_\pi)^2 + K_\pi (\partial\theta_\pi)^2] \\ + \int dx [g_{23} \cos \sqrt{8}\phi_\pi + g_4 \sin \sqrt{2}\theta_\pi], \quad (15)$$

where $g_{23} = g_2 + g_3$ and we have used the approximation $\langle\cos \sqrt{8}\phi_0\rangle \simeq \langle\cos \sqrt{2}\phi_0\rangle \simeq 1$. Note that the parameters in Eq. (15) should be regarded as renormalized ones under the renormalization group flow down to the above mentioned energy scale. In this Hamiltonian, the g_{23} -term favors the CDW state while the g_4 -term leads to the band insulator, and this competition can lead to a gapless state when these two perturbations cancel each other. The resulting gapless state is described by the $c = 1/2$ Majorana fermions, which corresponds to the criticality of the CDW phase transition from the band gapped Dirac state discussed in the previous section. To see this, we focus on a fine-tuned state where the two perturbation terms are maximally competing having the same scaling dimensions, $[g_{23}] = [g_4]$, namely

$$2K_\pi = \frac{1}{2K_\pi} \Rightarrow K_\pi = \frac{1}{2}. \quad (16)$$

By redefining the boson fields as $\phi'_\pi = \phi_\pi/\sqrt{K_\pi}$, $\theta'_\pi = \sqrt{K_\pi}\theta_\pi - \pi/4$ with $K_\pi = 1/2$, the Hamiltonian is rewrit-

ten as

$$H_{\text{eff}} = \frac{v_\pi}{2\pi} \int dx [(\partial\phi'_\pi)^2 + (\partial\theta'_\pi)^2] + \int dx [g_{23} \cos 2\phi'_\pi + g_4 \cos 2\theta'_\pi]. \quad (17)$$

This Hamiltonian is called the self-dual sine-Gordon model and has been studied extensively^{6,35–38}. Since the scaling dimensions of both g_{23}, g_4 -terms are 1, one can refermionize them by using a spinless fermion operator $\psi_r(x) \simeq \eta_r e^{-i(r\phi'_\pi - \theta'_\pi)}/\sqrt{2\pi a}$ as

$$\cos 2\phi'_\pi = -i\pi a [\psi_R^\dagger \psi_L - \psi_L^\dagger \psi_R], \quad (18a)$$

$$\cos 2\theta'_\pi = -i\pi a [\psi_R^\dagger \psi_L^\dagger - \psi_L \psi_R]. \quad (18b)$$

Therefore the self-dual sine-Gordon model is mapped to a free spinless fermion model with mass terms,

$$H_{\text{eff}} = \int dx -iv_\pi [\psi_R^\dagger \partial \psi_R - \psi_L^\dagger \partial \psi_L] - im_{23} [\psi_R^\dagger \psi_L - \psi_L^\dagger \psi_R] - im_4 [\psi_R^\dagger \psi_L^\dagger - \psi_L \psi_R], \quad (19)$$

where $m_{23} = \pi a g_{23}, m_4 = \pi a g_4$. Then we introduce Majorana fermions $\gamma^1 = (\psi + \psi^\dagger)/\sqrt{2}, \gamma^2 = (\psi - \psi^\dagger)/\sqrt{2}i$ to write the Hamiltonian in the Majorana basis,

$$H_{\text{eff}} = \sum_{a=1,2} \int dx -i \frac{v_\pi}{2} [\gamma_R^a \partial \gamma_R^a - \gamma_L^a \partial \gamma_L^a] - im_{\gamma a} \gamma_R^a \gamma_L^a, \quad (20)$$

where $m_{\gamma 1} = m_{23} + m_4, m_{\gamma 2} = m_{23} - m_4$. Clearly, only one Majorana fermion γ_2 is gapless and the other one γ_1 is gapped along the special line given by $m_{23} = m_4$ in the V - t_\perp plane. (Note that we have assumed $t_\perp > 0$ and thus $m_{\gamma 1} \neq 0$ in this study.) This emergent gapless Majorana fermions describe the $c = 1/2$ conformal field theory which is the critical theory for the CDW phase transition from the band gapped Dirac state studied in the previous section. Physically, the Majorana fermions correspond to domain walls of the CDW order.

We have shown within the bosonization how the fermionic criticality at the Gaussian transition is connected to the bosonic criticality at the Ising transition. These discussions are summarized in the global phase diagram shown in Fig. 10. We expect that competition between the band gap and interaction would be important also for higher dimensions. For example in spinless fermions on the two dimensional π -flux square lattice, there is a CDW quantum phase transition with (2+1)D chiral Ising criticality at $V = V_c > 0$ from the gapless Dirac semimetal^{9–12}, while a transition from the gapped Dirac insulator is expected to show 3D Ising criticality if it is continuous. The two phase transitions would be connected in a non-trivial way, and the familiar 3D Ising criticality might be understood as a critical state of an emergent object from the (2+1)D chiral Ising critical point. Further studies are necessary to develop theoretical understanding of these issues.

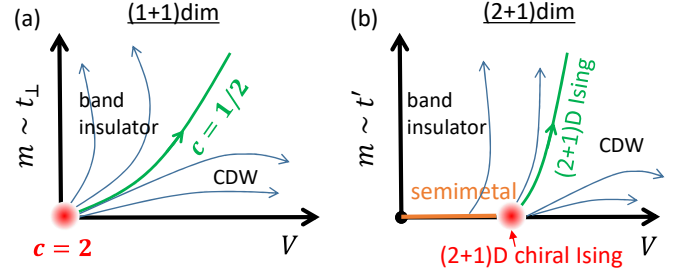


FIG. 10. (a) Schematic global phase diagram in the V - t_\perp plane in (1+1)D. The red point at the origin is the $c = 2$ Gaussian transition point, and the green curve is the $c = 1/2$ Ising transition line separating the band insulator and CDW state. The arrows correspond to the renormalization group flow in the effective low energy model. (b) Expected phase diagram in (2+1)D. t' is an additional hopping which induces a band gap.

III. SUMMARY AND DISCUSSION

We have studied the CDW quantum phase transition and its criticality in spinless fermions on the quasi one dimensional π -flux square lattice, by using iDMRG and bosonization. We find that the phase transition from a Dirac band insulator is continuous and its universality class is (1+1)D Ising with the central charge $c = 1/2$ when $L_y = 4n + 2 = 2, 6, \dots$ under the periodic boundary condition, while that from a Dirac semimetal is Gaussian with $c = 2$ when $L_y = 4n = 4, 8, \dots$. By introducing the twisted boundary condition, we discussed how the fermionic criticality of the Gaussian transition in the gapless Dirac semimetal is connected to the bosonic criticality of the Ising transition in the gapped Dirac band insulator. The global phase diagram was discussed, where the $c = 2$ critical point is connected to the $c = 1/2$ critical line. The resulting $c = 1/2$ critical line arises from the competition between the band mass and the density interaction leading to the CDW gap, and is described by the emergent Majorana fermions which is regarded as a fractionalized object. This could give a new insight for a comprehensive understanding of phase transitions in both metals and insulators. Our results could provide a basis to understand higher dimensional systems, and also may be directly relevant for the artificially created π -flux systems in cold atoms with the synthetic magnetic field^{39,40}.

ACKNOWLEDGEMENT

We are grateful to Y. Fuji for valuable discussions and constructive comments on our manuscript. We also thank J. -H. Chen, R. Kaneko, M. Nakamura, M. Oshikawa, S. Takayoshi and Y. Yao for fruitful discussions. The numerical calculations have been done at Max Planck Institute for the Physics of Complex Systems. This work was supported by Grants-in-Aid for

-
- * tada@issp.u-tokyo.ac.jp
- ¹ T. Moriya and K. Ueda, *Advances in Physics* **49**, 555 (2000).
 - ² H. v. Löhneysen, A. Rosch, M. Vojta, and P. Wölfle, *Rev. Mod. Phys.* **79**, 1015 (2007).
 - ³ M. Brando, D. Belitz, F. M. Grosche, and T. R. Kirkpatrick, *Rev. Mod. Phys.* **88**, 025006 (2016).
 - ⁴ E. Berg, S. Lederer, Y. Schattner, and S. Trebst, *Annual Review of Condensed Matter Physics* **10**, 63 (2019).
 - ⁵ T. Giamarchi, *Quantum Physics in One Dimension* (Oxford University Press, 2003).
 - ⁶ A. O. Gogolin, A. A. Nersesyan, and A. M. Tsvelik, *Bosonization and Strongly Correlated Systems* (Cambridge University Press, 2004).
 - ⁷ S. Sorella and E. Tosatti, *Europhysics Letters (EPL)* **19**, 699 (1992).
 - ⁸ F. F. Assaad and I. F. Herbut, *Phys. Rev. X* **3**, 031010 (2013).
 - ⁹ L. Wang, P. Corboz, and M. Troyer, *New Journal of Physics* **16**, 103008 (2014).
 - ¹⁰ L. Wang, Y.-H. Liu, and M. Troyer, *Phys. Rev. B* **93**, 155117 (2016).
 - ¹¹ Z.-X. Li, Y.-F. Jiang, and H. Yao, *Phys. Rev. B* **91**, 241117 (2015).
 - ¹² Z.-X. Li, Y.-F. Jiang, and H. Yao, *New Journal of Physics* **17**, 085003 (2015).
 - ¹³ F. Parisen Toldin, M. Hohenadler, F. F. Assaad, and I. F. Herbut, *Phys. Rev. B* **91**, 165108 (2015).
 - ¹⁴ Y. Otsuka, S. Yunoki, and S. Sorella, *Phys. Rev. X* **6**, 011029 (2016).
 - ¹⁵ Z. Zhou, C. Wu, and Y. Wang, *Phys. Rev. B* **97**, 195122 (2018).
 - ¹⁶ P. Corboz, P. Czarnik, G. Kapteijns, and L. Tagliacozzo, *Phys. Rev. X* **8**, 031031 (2018).
 - ¹⁷ B. Rosenstein, H.-L. Yu, and A. Kovner, *Physics Letters B* **314**, 381 (1993).
 - ¹⁸ L. Rosa, P. Vitale, and C. Wetterich, *Phys. Rev. Lett.* **86**, 958 (2001).
 - ¹⁹ I. F. Herbut, *Phys. Rev. Lett.* **97**, 146401 (2006).
 - ²⁰ I. F. Herbut, V. Juričić, and O. Vafek, *Phys. Rev. B* **80**, 075432 (2009).
 - ²¹ L. Janssen and I. F. Herbut, *Phys. Rev. B* **89**, 205403 (2014).
 - ²² B. Ihrig, L. N. Mihaila, and M. M. Scherer, *Phys. Rev. B* **98**, 125109 (2018).
 - ²³ D.-H. Lee, *Phys. Rev. Lett.* **107**, 166806 (2011).
 - ²⁴ M. Hohenadler, Z. Y. Meng, T. C. Lang, S. Wessel, A. Muramatsu, and F. F. Assaad, *Phys. Rev. B* **85**, 115132 (2012).
 - ²⁵ S. R. White, *Phys. Rev. Lett.* **69**, 2863 (1992).
 - ²⁶ U. Schollwöck, *Rev. Mod. Phys.* **77**, 259 (2005).
 - ²⁷ U. Schollwöck, *Annals of Physics* **326**, 96 (2011), january 2011 Special Issue.
 - ²⁸ I. P. McCulloch, arXiv:0804.2509.
 - ²⁹ J. A. Kjäll, M. P. Zaletel, R. S. K. Mong, J. H. Bardarson, and F. Pollmann, *Phys. Rev. B* **87**, 235106 (2013).
 - ³⁰ J. Hauschild and F. Pollmann, *SciPost Phys. Lect. Notes*, 5 (2018).
 - ³¹ P. Calabrese and J. Cardy, *Journal of Statistical Mechanics: Theory and Experiment* **2004**, P06002 (2004).
 - ³² L. Balents and M. P. A. Fisher, *Phys. Rev. B* **55**, R11973 (1997).
 - ³³ S. T. Carr, B. N. Narozhny, and A. A. Nersesyan, *Phys. Rev. B* **73**, 195114 (2006).
 - ³⁴ Y.-C. He, M. P. Zaletel, M. Oshikawa, and F. Pollmann, *Phys. Rev. X* **7**, 031020 (2017).
 - ³⁵ D. G. Shelton, A. A. Nersesyan, and A. M. Tsvelik, *Phys. Rev. B* **53**, 8521 (1996).
 - ³⁶ D. G. Shelton and A. M. Tsvelik, *Phys. Rev. B* **53**, 14036 (1996).
 - ³⁷ P. Lecheminant, A. O. Gogolin, and A. A. Nersesyan, *Nuclear Physics B* **639**, 502 (2002).
 - ³⁸ N. J. Robinson, A. Altland, R. Egger, N. M. Gergs, W. Li, D. Schuricht, A. M. Tsvelik, A. Weichselbaum, and R. M. Konik, *Phys. Rev. Lett.* **122**, 027201 (2019).
 - ³⁹ J. Dalibard, F. Gerbier, G. Juzeliūnas, and P. Öhberg, *Rev. Mod. Phys.* **83**, 1523 (2011).
 - ⁴⁰ T. Ozawa and H. M. Price, *Nature Review Physics* **1**, 349 (2019).